Title: Aberrant BCMA Signaling Promotes Tumor Growth by Altering Protein Translation Machinery, a Therapeutic Target for the Treatment of Relapse/Refractory Multiple Myeloma

Authors: Yu Rebecca Miao[1], Can Cenik[2], Dadi Jiang[3], Kazue Mizuno[1], Grace Caiyun Li[1], Hongjuan, Zhao[1,4], Kaushik Thakker[1], Anh Diep[1], Jimmy Yu Xu[1], Xin Eric Zhang[6], Michaela Liedtke[5], Parveen Abidi[5], Wing-sze Leung[1], Albert C. Koong[3], Amato J. Giaccia[1,6]*

Affiliations:

[1]Department of Radiation Oncology, Stanford University; Stanford, CA 94305, USA.

[2]Department of Molecular Biosciences, University of Texas at Austin; Austin, TX 78712, USA.

[3]Department of Radiation Oncology, MD Anderson Cancer Center; Houston, TX 77030, USA.

[4]Department of Urology, Stanford University; Stanford, CA 94305, USA.

[5]Department of Medicine (Hematology), Stanford University, Stanford, CA 94305, USA.

[6]Department of Oncology, Oxford Institute for Radiation Oncology, University of Oxford; Oxford, OX3 7DQ, UK.

*Corresponding Author. Email: giaccia@stanford.edu, amato.giaccia@oncology.ox.ac.uk.

One Sentence Summary: B-Cell Maturation Antigen is a regulator of protein translation machinery in Multiple Myeloma and can be safely targeted as a treatment for relapse/refractory Multiple Myeloma.

ABSTRACT

B-cell maturation antigen (BCMA) is critical for the viability of Multiple Myeloma (MM) tumor cells and targeting BCMA poses a remarkable opportunity as a potential therapeutic in this cancer. Recent approval of BCMA directed CAR-T and Antibody-Drug-Conjugates (ADCs) have revolutionized MM treatment landscape. Despite such clinical success, treatment resistance and dose limiting toxicity remain as major clinical challenges. Using ribosome profiling, we established a molecular link between BCMA signaling inhibition and protein translation machinery. In addition, BCMA signaling alters the translation efficiency of a transcriptional regulator ATMIN without changing the total mRNA transcript level. Furthermore, ATMIN can transcriptionally regulate IL-6, a critical survival factor for MM. To inhibit the BCMA signaling pathway, we devised both genetic knockdown strategy and pharmacological inhibition by using a soluble BCMA decoy receptor fusion protein (sBCMA-Fc) to trap both of its ligands, APRIL and BAFF. We demonstrated that treatment of MM tumor cells with sBCMA-Fc inhibits tumor progression in numerous *in vivo* and syngenic PDX tumors models without significant adverse effects. Furthermore, the addition of sBCMA-Fc treatment can restore bortezomib sensitivity in previously bortezomib resistant MM tumors, further adding to its therapeutic value in the treatment of relapse /refractory MM patients. Inhibiting BCMA signaling through neutralization of its ligands APRIL and BAFF with a sBCMA-Fc fusion protein represents a safe and efficacious treatment strategy for the treatment of relapse and refractory MM.

INTRODUCTION

Multiple Myeloma (MM) remains incurable and despite current therapies, patients often experience treatment relapse and succumb to the disease (1, 2). The development of CAR-T therapies and Antibody-Drug Conjugates (ADC) directed at B-Cell Maturation Antigen (BCMA) have enjoyed considerable clinical success with a subset of patients reporting complete remission post-treatment (3-5). However, treatment relapse and dose limiting toxicity remain as major clinical challenges in this group of patients (6-8). Additionally, elderly patients were often excluded from both CAR-T and ADC treatments due to their poor overall health, representing a critically unmet clinical need within this population (9, 10). Therefore, new efficacious therapeutics with favorable safety and tolerability profiles are needed for treating patient's ineligible for both frontline and new investigational MM therapies associated with high drug related toxicity.

B-Cell Maturation Antigen (BCMA) is a member of the TNF receptor family that is uniquely expressed on plasma cells and some differentiated B cells (11, 12). Although widely accepted as a marker of MM and a selective cell surface target for MM targeted therapies, BCMA signaling is also essential for the growth and survival of MM cells (13-15). Upon April or BAFF binding, BCMA promotes AKT, MAPK, and NF-κB signaling, facilitating the transcriptional increase of pro-tumor cytokines that lead to osteoclast mediated bone degradation, cell adhesion and angiogenesis within the tumor niche, promoting MM progression and relapse (16, 17). Taken together, these data present a strong case to target BCMA signaling in addition to targeting BCMA at the cell surface in the bone marrow microenvironment for the treatment of MM.

Functionally, the loss of BCMA signaling leads to apoptosis and MM cell death (18, 19). However, little is known about the regulation of downstream pathways after activation of BCMA signaling

in MM cells, especially at the translational level. In this study, we investigated the role of BCMA in regulating protein translation and whether changes in protein translation of specific mRNAs are tightly linked to MM progression. In MM, tumor and stromal derived pro-tumor cytokines are associated with creating oncogenic tumor microenvironments that promote tumor growth by favoring osteolytic bone degradation, inhibiting apoptosis and promoting drug resistance (20-23).

A different approach to therapeutically block BCMA signaling is to trap both ligands of BCMA, A proliferation-inducing ligand (APRIL) and B-cell activating factor (BAFF) using a ligand trap fusion protein of the extracellular domain of BCMA fused to an IgG Fc (sBCMA-Fc). The APRIL ligand binds to BCMA with a high binding affinity in a trimeric form and stimulates B cell proliferation. In contrast, BAFF, binds BCMA with a weaker affinity. Interestingly, higher serum BAFF levels compared to serum ARPIL levels are found in MM patients, possibly to compensate for its weaker affinity (17, 24).

In this study, we identified BCMA as a critical regulator of protein translation and in particular the translational efficiency of ATMIN, leading to altered IL-6 production. We also investigated the effect of inhibiting BCMA signaling by sBCMA-Fc on tumor progression in numerous *in vivo* and syngenic PDX tumors models. Interestingly, the addition of sBCMA-Fc treatment can restore bortezomib sensitivity in previously bortezomib resistance MM tumors, further adding to its therapeutic value in the treatment of relapse and refractory (r/r) MM patients. Thus, targeting BCMA signaling through neutralization of its ligands APRIL and BAFF using sBCMA-Fc presents as a safe and efficacious treatment strategy for the treatment of MM.

RESULTS

BCMA Signaling is Essential for the Growth and Survival of Multiple Myeloma.

To investigate whether BCMA is dysregulated in Multiple Myeloma, BCMA mRNA levels were evaluated in both healthy plasma cells and myeloma cells obtained from healthy volunteers and MM patients, respectively. BCMA expression was significantly elevated in patient myeloma cells compared to healthy plasma cells (Fig. 1A). When examining BCMA mRNA expression in a panel of cancer cells originated from different tissue types in the Oncomine database, BCMA was found to be uniquely elevated on MM and B-cell lymphoma, but not detectable in cancer cells other than those of a B cell origin (Sup. Fig. 1A). To examine whether the two major ligands of BCMA were elevated in MM patients, serum levels of APRIL (Fig. 1B) and BAFF (Fig. 1C) were evaluated in the peripheral blood of both healthy individuals and MM patients by ELISA. We found significantly higher levels of APRIL and BAFF in the serum of MM patients, consistent with previous reports that elevated levels of APRIL and BAFF were detected in MM patients and are associated with poor overall survival (25, 26).

To test the dependency of MM proliferation on BCMA signaling, BCMA was genetically inhibited in MM cells using siRNA. BCMA knockdown resulted in decreased MM cell growth and cell death over a period of 72 hours (Sup. Fig 1B, 1C). Since stable knockdown of BCMA in MM cells resulted in cell death, a Tet-off doxycycline-controlled BCMA stable KD system (dox shBCMA) was introduced into MM cell lines INA-6 and MM1.R to investigate the consequences of BCMA knockdown in tumors (Sup. Fig. 1D). Mice inoculated with dox shBCMA MM cells were provided with doxycycline containing water at the dose of 5 mg/ml. Loss of BCMA led to significant reduction in tumor growth in both INA-6 (Fig. 1D, E), and MM1.R (Sup. Fig 1F) MM models. In doxycycline induced MM tumors, cell proliferation was significantly diminished as evident by

decreased Ki67 signals (Fig. 1F, G. Sup Fig. 2A, B) and apoptosis was increased as detected by the TUNEL assay (Fig. 1H, 1I, Sup. Fig. 2C, D). To investigate the proteomic changes that occur upon loss of BCMA signaling, we performed Reverse Phase Protein Array (RPPA) on U266 MM cells after siBCMA treatment and found changes in the signaling cascade associated with protein translation such as the mTOR, p70SK6, and 4EBP1 mediated signaling pathways, suggesting a potential link between BCMA signaling and protein translation (Sup. Fig. 1C, Data Table S1). The regulation of BCMA on critical components of the translational machinery were validated by western analysis in U266 MM cell lines before and after BCMA siRNA (Sup. Fig. 1C). Since elevated levels of pathological immunoglobulin levels (M protein or paraprotein) is a hallmark feature of MM, we investigated human M protein levels secreted by human MM tumors. A significant reduction in serum M protein levels in mice bearing dox-inducible shBCMA xenograft MM tumors was observed (Fig. 1J). Since the presence of M protein signifies the production of dysregulated immunoglobulin proteins in myeloma cells and is a hallmark of MM progression (27), we thought that this observation warranted a further investigation into the potential association between BCMA signaling and protein production and secretion in MM.

Ribosome Profiling Reveals Distinct Changes in Protein Translation Upon BCMA Signaling Alteration

Dis-regulated protein translation in Multiple Myeloma leads to increased production and secretion of M proteins that is associated with detrimental pathological consequences in MM patients. In this study, inhibition of BCMA was associated with a decreased activity of signaling associated with protein translation and reduction in the total serum M protein (Fig. 1J, Sup. Fig. 1C). To further investigate the relationship between BCMA signaling and protein translation, we

performed ribosome profiling on U266 MM cell line to evaluate the gene-specific changes in translational efficiency upon the loss of BCMA signaling using siBCMA. Briefly, mRNA fragments protected by ribosomes were isolated and sequenced along with quantification of total RNA abundance with RNA-Seq (28). The joint analysis of this data provides a quantitative measure of gene-specific translation efficiency (Fig. 2A). First, we carried out extensive quality control analysis of the ribosome profiling data using the RiboR (29). In particular, we observed the expected three nucleotide periodicity, enrichment of footprints in coding regions and the expected signals at the translation start and stop sites (Sup. Fig. 3B, C). Spearman correlation showed robust correlation between all samples with the exception of BCMA Scramble 3 (RPF3) (Sup. Fig 3D). Therefore, RPF3 was removed from analysis to retain the quality and consistency of the reads (Sup Fig. 3E).

We first profiled changes in the total mRNA expression in siBCMA MM cells compared to the siScramble as reference for translation efficiency (Data Table S2. Sup. 3F, G). Ingenuity Pathway Analysis (IPA) identified mTORC1 mediated signaling as the top canonical pathways altered upon the loss of BCMA signaling activity, and this finding was consistent with western blotting and RPPA analysis done earlier (Fig. 2B, Sup. Fig 1C, 3H). Similarly, GeneGo MetaCore^{TM} analysis identified enrichment in protein translation associated EIF2 signaling pathway as the top process networks altered upon loss of BCMA (Fig. 2C). These findings further validated our hypothesis that the loss of BCMA signaling can suppress protein translation in MM cells. Subsequently, we calculated changes in translation efficiency when controlling for differences in total mRNA expression (Data Table S3, Fig. 2D) (30). Once again, we identified targets that are associated with protein translation machinery, some of which were consistent with total mRNA transcript readouts. Using gene enrichment analysis database REACTOME, we identified enriched gene signatures

associated with protein translation, initiation and elongation upon loss of BCMA expression (Fig. 2E-G). Furthermore, protein signatures that are responsible for the synthesis of both large and small ribosome subunits were also decreased upon the loss of BCMA expression in MM cells, suggesting a potential role of BCMA signaling in ribosome function and integrity (Fig. 2G). Collectively, these data suggest that BCMA signaling in MM cells maybe a critical regulator of protein translation machinery both at transcription and translation level.

Taken together, genome-wide ribosome profiling and RNA sequencing analysis identifies BCMA as a critical regulator of MM protein translation. Therefore, the reduction in M protein secretion (Fig. 1J) is likely due to decreased protein translation as a result of BCMA loss.

BCMA Signaling Regulates IL-6 Expression Through Modulating the Translation Efficiency of ATMIN

A unique feature of ribosome profiling is its ability to capture the position and density of a full set of ribosomes that are actively engaged in translation along the coding sequence. In this study, we used ribosome profiling to identify targets with altered translation efficiency without changes in the total mRNA transcript abundance. Upon analysis, we identified ATMIN (ASCIZ) as a previously unreported downstream translational target of BCMA (Fig. 3A). To experimentally validate the translational changes in ATMIN expression upon loss of BCMA, we performed polysome fractionation analysis. Ribosomes captured from MM cell lysates are separated into pooled fractions of heavily translated polysomes, lighter ribosomes and monosomes and analyzed to determine the translation efficiency of ATMIN upon the loss of BCMA expression (Fig. 3B). When compared to the control, BCMA KD MM cells showed significantly decreased levels of ATMIN transcript binding to heavily translated polysomes, which is indictive of reduced ATMIN

translation efficiency (Fig. 3C). Furthermore, we validated our findings from ribosome profiling analysis that ATMIN is regulated exclusively at the translational level since total ATMIN mRNA transcripts remain unchanged upon the loss of BCMA expression (Fig. 3D).

While initially discovered as an ATM interacting protein, ATMIN is often associated with ATM-mediated signaling and recruitment of 53BP1 upon DNA damage (31-33). However, since we did not observe changes in 53BP1 expression in the Reverse Phase Protein Array (RPPA) upon genetic inhibition of BCMA in MM cells, we hypothesize that the altered ATMIN expression here may not be a result of DNA damage response (Data Table S1). Alternatively, ATMIN has been reported to function as a transcription regulator to transcriptionally regulate Dynein light chain (*Dynll1)* and facilitate the development and progression of B cell lymphoma, another cancer of B-cell origin (34-37). In determining which critical downstream targets of ATMIN are implicated in MM cells, we found that the pro-inflammatory cytokine IL-6 is transcriptionally regulated through ATMIN. Both siBCMA and ATMIN CRISPR knockout led to reduced IL-6 expression at the mRNA and protein levels, indicating that ATMIN is regulating the expression of Il-6 at the transcriptional level (Fig. 3E-G. Sup Fig. 4A). Functionally, this change in IL-6 expression is also consistent with decreased secreted levels of IL-6 in the supernatant of MM cells upon the loss of ATMIN (Fig. 3H). Since IL-6 is known to be a critical driver of MM disease both experimentally and clinically, we determined whether the activation of ATMIN mediated increase IL-6 secretion can activate human IL-6 receptor (IL-6R) and its subsequence signaling cascade. We stably introduced a doxycycline inducible ATMIN expression vector into a HEK293 derived IL-6 reporter cell called HEK-Blue^{tm} IL-6 (commercially available through InvivoGen US). The HEK-Blue^{tm} IL-6 Cells were generated by stable transfection of HEK293 cells with the genes encoding human IL-6 receptor (IL-6R) and signal transducer and activator of STAT3, a classic downstream effector of

IL-6/IL-6R signaling. Cells were further transfected with a STAT3 inducible secreted embryonic alkaline phosphatase (SEAP) reporter gene. This allows the quantification of IL-6 mediated STAT3 signaling activation using a colorimetric reagent that detects SEAP report activity. Here, we observed an approximately 5-fold-increase of IL-6R activity upon the induction of ATMIN compared to HEK-Blue^{tm} IL-6/ATMIN cells without doxycycline induction (Fig. 3I). Since this reporter system has been tested by the manufacturer to be highly specific to IL-6 mediated signaling activation, we propose that ATMIN can promote the expression and activity of IL-6 signaling pathway.

Soluble BCMA Decoy Receptor Inhibits APRIL and BAFF Induced BCMA Signaling in MM Cells

To determine the effect of inhibiting APRIL and BAFF ligands binding to BCMA on MM growth and viability, we generated a recombinant fusion decoy receptor comprised of the Extracellular Domain (ECD) of the BCMA receptor linked to a human IgG1 Fc domain (sBCMA-Fc) for improved pharmacokinetic and pharmacodynamic properties (38). Soluble BCMA is capable of binding both APRIL and BAFF, preventing subsequent ligand-receptor signaling activation. The sBCMA-Fc molecule was tested *in vivo* using an Adeno-Associated Virus (AAV) approach (Fig. 4A. Sup. Fig. 4B). In this experimental approach, an AAV viral vector incorporating mouse IgG Fc (sBCMA-Fc) or IgG Fc control was administered intravenous in mice inoculated with MM1.R MM xenografts (Fig. 4B). We observed a significant decrease in tumor growth in the sBCMA-Fc group compared to the Fc only control, supporting the critical roles of APRIL and BAFF in promoting MM growth and survival (Fig. 4C). To make these studies more translationally applicable, we generated recombinant human sBCMA-Fc protein that could be used both *in vitro*

and *in vivo* (Fig. 4D). Based on Surface Plasmon Resonance (SPR Biacore®) analysis, the binding constant (K_D) of sBCMA-Fc to APRIL is $1.01x10^{-10}$ M and to BAFF is $4.03x10^{-10}$ M (Fig 4E, 4F). Interestingly, while the K_D between APRIL and sBCMA-Fc was similar to what was previously reported (39), binding to BAFF was significantly higher compared to previously reported studies.

To determine the inhibitory effect of sBCMA-Fc on the viability of MM cell lines, we performed *in vitro* cytotoxicity assays using U266 and MM1.R cell lines. A reduction in MM cell viability was only observed when cells were cultured in reduced serum conditions, suggesting the presence of growth factors and/or cytokines such as IL-6 within the fetal calf serum maybe capable of supporting MM cell growth in the absence of BCMA signaling while this cell culture effect was not observed *in vivo* (Fig 4G). Apoptosis of MM cells post sBCMA-Fc treatment was also visualized through electron microscopy in a dose dependent manner (Fig 4H). Mechanistically, the downstream effectors of BCMA signaling were also interrogated at the protein level in a time dependent manner when cells were treated with 10 ng/ml of sBCMA-Fc. Consistent with our genetic inhibition studies, we saw decreased protein expression of pMAPK, pAKT and phospho-mTOR mediated signaling as well as a reduction in both ATMIN and IL-6 expressions (Fig 4I). Since the reduction of ATMIN protein levels was also observed in MM cells treated with sBCMA-Fc, we further validated the secreted levels of IL-6 in MM cell supernatants. Consistent with previous findings, treatment with 10 ng/ml of sBCMA-Fc led to an approximately 3-fold and 2-fold reduction of IL-6 secretion in U266 and MM1.R MM cell lines respectively (Fig. 4J). This is likely to be caused by decreased ATMIN activity as a result of BCMA signaling inhibition.

We also investigated the *in vivo* efficacy of sBCMA-Fc in a number of MM models. First, the pharmacokinetic profile of sBCMA-Fc was determined by administering 10 mg/kg of fluorescently labeled sBCMA-Fc into non-tumor bearing mice and monitoring the fluorescent

intensity over 72 hours. A half-life of approximately 24 hours was determined by monitoring changes in signal intensity (Fig. 5A). Additionally, serum levels of mouse APRIL and BAFF were examined over a period of 4 days after the administration of a single dose of 10 mg/kg sBCMA-Fc. While sBCMA-Fc was capable of suppressing both APRIL and BAFF in serum, we observed longer inhibition of serum BAFF levels compared to APRIL levels (Fig. 5B). Subsequently, the anti-tumor activities of sBCMA-Fc were tested in two subcutaneous xenograft MM models, MM1.R and INA-6. Treatment with sBCMA-Fc resulted in significant tumor reduction in both xenograft models (Fig 5C, D) and was associated with both decreased tumor cell proliferation (Fig. 5E) and increased apoptosis (Fig. 5F). To test the anti-tumor activity of sBCMA-Fc in more clinically relevant models, we established MM PDX orthotopic models using myeloma cells isolated from MM patient bone marrow biopsies. Out of the eleven patient biopsies collected, we successfully engrafted two PDX lines through *in vivo* serial passage. Treatment with sBCMA-Fc was initiated upon confirming successful engraftment by detecting the presence of human M protein in the serum (Fig. 5G). Additionally, bone CT scans were performed on animals with confirmed human M protein in circulation. Mice with successful engraftment showed macroscopic osteolytic lesions that are consistent with clinical representation of widespread osteopenia in MM patients (Fig. 5H). A total of fourteen-10 mg/kg doses of sBCMA-Fc were administered every 48 hours for a period of 28 days and tumor growth was monitored through serum M protein levels until mice reach a terminal endpoint. Treatment with sBCMA-Fc led to a significant reduction of tumor growth and M protein over time in two separate MM PDX models, further validating the anti-tumor activity of sBCMA-Fc in a clinically translatable setting (Fig. 5I and 5J).

Inhibition of the APRIL/BAFF-BCMA Signaling Pathway Leads to Bortezomib Re-Sensitization in Multiple Myeloma.

The heterogeneous nature of MM often leads to the emergence of both intrinsic and acquired resistance to standard of care treatments, and relapse is the unfortunate reality for most MM patients (40, 41). Bortezomib, a protease inhibitor currently included in MM treatment regimens shows clinical activity initially, but treatment resistance and disease relapse occur over time. We hypothesized that BCMA signaling may play a role in acquired bortezomib resistance. To test this hypothesis, we developed a panel of bortezomib resistant MM cell lines by continuously exposing cells to gradually increasing concentrations of bortezomib. This treatment regimen resulted in more than a 3-folds increase in the survival of resistant cells compared to their parental counterparts to bortezomib (Fig. 6A). MM cells resistant to bortezomib possessed elevated BCMA expression, suggesting a potential association between BCMA signaling and bortezomib resistance (Fig. 6B, 6C).

In vitro cytotoxicity assays demonstrated enhanced survival of bortezomib resistant MM cells compared to parental, non-bortezomib resistance MM cells treated with 5 or 10 nM of bortezomib (Fig. 6D, E). However, treatment with sBCMA-Fc along also lead to a significant reduction in the growth of bortezomib resistant MM cells (Fig. 6F). Importantly, the combination treatment of bortezomib and sBCMA-Fc reduced the survival advantage of bortezomib resistant MM cells, suggesting that the addition of sBCMA-Fc can effectively re-sensitize bortezomib resistant cells to bortezomib treatment (Fig. 6G). To evaluate whether similar therapeutic effect can also be established *in vivo*, bortezomib resistant MM1.R MM cells were subcutaneously inoculated into NSG mice and were treated with vehicle alone, sBCMA-Fc at 10mg/kg every 48 hours, daily dosing of bortezomib at 0.5mg/kg or the combination of sBCMA-Fc and bortezomib. Kaplan Meir

survival analysis was carried out as animals were sacrificed once tumors reached a maximal size that requires ethical termination. Consistent with *in vitro* analysis, animals that received the combination treatment showed a significant survival advantage, with 80% of animals remaining disease free up to 100 days (Fig. 6H). sBCMA-Fc also significantly improved median survival from 35 days in the control group to 67 days. As expected, the bortezomib alone treated group failed to show therapeutic benefit when compared to the control. Finally, to determine normal tissue toxicity of sBCMA-Fc, non-tumor bearing mice were dosed with sBCMA-Fc at 10mg/kg every 48 hours continuously for 28 days. No significant changes in body weight, hematological or tissue toxicity were identified in animals treated with sBCMA-Fc, providing evidence that sBCMA-Fc can be used as a monotherapy or safely added to current standard-of-care MM treatment to enhance therapeutic efficacy without additional toxicity (Fig. 6I. Sup. Fig 4C, D).

DISCUSSION

The rapid emergence of drug-resistant clones in MM patients with persistent minimal residue disease (MRD) or even MRD-negative patients leads to treatment relapse or refractory disease (42, 43). Clinically, the overall survival of patients with r/r MM after protease inhibitors, Immunomodulating drugs (IMiD) and targeted therapeutic antibody treatment is extremely low (44). While the addition of BCMA-targeting ADCs and CAR-Ts to the MM treatment landscape have provided high hopes for curing this devastating disease, clinical challenges associated with treatment relapse and intolerable drug-mediated toxicity still occurs, therefore demanding the need for the developing much safer and efficacious therapies to treat r/r Multiple Myeloma.

Results from our studies and others all have reported seeing significantly elevated BCMA expression in MM patients compared to healthy plasma cell donor (45). The activation of BCMA

pathway in MM is through the binding of its ligands, APRIL and BAFF, resulting in pro-survival signals that promotes the progression of MM diseases (17, 26). While it is well established that the BCMA signaling activation provides MM cells with essential growth and survival advantages, little is known about the specific biological sequences that leads to such outcome. In this study, we took an unique approach using ribosome profiling analysis to examine the global translational changes in MM cells upon the loss of BCMA. This strategy allows us to reveal distinctive molecular signatures that underwent post-transcriptional alteration, which otherwise cannot be detected by measuring total mRNA transcripts (30, 46). Upon analysis, we found enrichment in the molecular signatures that governs protein translation machineries, including translation initiation, elongation and ribosome integrity. Indeed, the translation of mRNA into functional protein is essential to virtually every cellular process and thus is highly regulated, this is especially true for plasma cells, which serves as the central hub of immunoglobulin production. Consistent with our previous findings, the loss of BCMA resulted in the reduction of total human M protein in animals inoculated with human MM tumors, which at high levels, is clinically associated with infections, peripheral neuropathy and bone damages in MM patients (27, 47).

When ribosomes bound mRNA fragments are sequenced and mapped to its corresponding total mRNA transcriptome, one can numerically quantify the translation efficiency of the protein of interest. Here, for the first time, we showed ATMIN (ASCIZ) as one of the top candidates that is associated with changes in translation efficiency. ATMIN is commonly known as an ATM-interacting protein and is involved in DNA damage response (32). However, since DNA damage response pathways were not significantly altered upon loss of BCMA in our study, we propose that ATMIN activation here is independent of DNA damage response. Alternatively, studies reported the direct interaction between ATMIN and dynein light chain subunit Dynll1 in an ATM

independent manner (35, 36). Specifically, while there are no published report investigating the association between ATMIN/Dynll1 activation in MM pathology, ATMIN and Dynll1 interaction has being shown to promote the development of B-cell lymphoma, a cancer type that is related to MM and provides important rationale for further investigating ATMIN signaling in MM (35).

We then further demonstrated a biological relationship between ATMIN and pro-inflammatory cytokine IL-6, where IL-6 can be transcriptionally regulated by BCMA signaling through ATMIN. IL-6 is a potent inducer of MM cell proliferation and survival (22). While mutilple IL-6 inhibitors were developed and tested in clinical trials as early as 1990s. Unfortunately, therapeutic agents targeting IL-6 have yet to show satisfactory anti-tumor efficacy in large randomized clinical trials (48). Multiple factors can contribute to the lack of efficacy observed in these IL-6 inhibitor trials. Most likely, the heterogeneity nature of MM allows cancer cells to clonally evolve and become IL-6 independent in the presence of selective pressure. Being an upstream regulator of IL-6, the inhibition of BCMA signal may prove to be more attractive as a therapeutic target than pharmacological suppression of IL-6. Interestingly, IL-6 is also known stimulate the production of APRIL in myeloid precursors through autocrine signaling, thus generating a positive feedback loop to maintain the growth and survival of MM cells (17).

In recent years, BCMA has been the subject of intense study for the treatment of MM and other B cell malignancies. BCMA targeting CAR-T therapies and BCMA directed ADCs have shown promising anti-tumor efficacy many recent clinical trials, but again treatment relapse and significant toxicity profiles strictly limits patient eligibility to those with excellent overall physical performance status, thus excluding heavily pre-treated, frail and elderly patients with r/r diseases (3, 7, 49). Additionally, therapeutic antibodies directly against BCMA receptor or its ligand APRIL have proven to be challenging with limited clinical success. We believe two major issues may

contribute to these challenges. First, therapeutic antibodies usually with nanomolar binding affinity often do not possess sufficient affinities required to disrupt the interaction between the native APRIL/BCMA binding, which is known to be in high picomolar. Second, APRIL neutralizing antibodies are not designed to block the interaction between BAFF and BCMA, leaving BCMA signaling partially active even in the absence of APRIL. To overcome these shortcomings, we propose to use recombinant soluble BCMA decoy receptor fusing to human IgG1 Fc domain as a ligand trap to both APRIL and BAFF. This approach allows us to take advantage of high binding affinity between APRIL and BCMA and enhance it further through the addition of IgG1 Fc. Although the native binding affinity between BAFF and BCMA is reported to be low in mM range, with the addition of the IgG1 Fc, we determined that the sBCMA-Fc has an improved binding to BAFF at 4.03×10^{-10}M. More importantly, *in vivo* pharmacodynamic studies showed almost complete suppression of serum APRIL and BAFF in mice upon administering a single dose of sBCMA-Fc at 10mg/kg. Suggesting that sBCMA-Fc is equally capable of inhibiting both human and mouse derived APRIL and BAFF. Consistent with these findings, sBCMA-Fc mediated suppression of APRIL and BAFF led to the inhibition of BCMA signaling in MM tumor, effectively reducing tumor growth in both xenograft and PDX models of MM. Furthermore, our studies have demonstrated that the addition of sBCMA-Fc to bortezomib treatment can effectively re-sensitize bortezomib resistant MM cells both *in vitro* and *in vivo*. Significantly prolonging the overall survival of animals inoculated with bortezomib resistant MM tumors without additional toxicity. Results from these studies provided sound preclinical rationale demonstrating that the inhibition of BCMA signaling axis by blocking ligands mediated interaction is a clinically feasible approach for targeting r/r MM.

We do recognize there are two potential shortcomings of this study that warrant further investigation. First, while we identified the involvement of ATMIN in MM and as a downstream target of BCMA in a translation dependent manner, the mechanistic association between ATMIN and IL-6 transcription activation in MM requires further study and will be the subject of interest for our next study. Second, both APRIL and BAFF are ligands to two other receptors TACI and BAFF-R with different binding affinities and structural conformations, further investigations are required to evaluate the biological changes downstream of TACI and BAFF-R on B cells upon the neutralization of APRIL and BAFF using sBCMA-Fc decoy receptor.

In this study, we established a molecular link between BCMA signaling and protein translation machinery, contributing to the fundamental understanding of the biological consequences associated with BCMA signaling. Furthermore, we identified ATMIN as a downstream translational target of BCMA signaling which led to the activation of IL-6. Therapeutically, the intervention of BCMA signaling in MM can be achieved through the use of sBCMA-Fc decoy receptor capable of augmenting APRIL and BAFF mediated BCMA activation. Overall, we propose that sBCMA-Fc is a viable clinical strategy that can be safely used as a treatment for Multiple Myeloma or added on to current SOC for the treatment of MM without additional toxicity.

MATERIAL AND METHODS

Study design

This study was designed to characterize the biological functionality of BCMA signaling during MM progression both experimentally and therapeutically. All Multiple Myeloma patient specimens were collected from Multiple Myeloma patients undergoing treatment at Stanford Cancer Center under the approval of Stanford IRB No.13535. Healthy blood specimens were

obtained from Stanford Blood Center. *In vivo* animal studies were conducted under the approval of AAAPLAC at Stanford University. Sample sizes for animal studies were determined based on power calculations done on similar *in vivo* studies in previous studies. All animals were randomly assigned to treatment groups. Samples were not excluded from studies except for animals that required early termination due to unforeseeable illness that is unrelated to the study. Endpoints of experiments were defined in advance for each experiment. Tumor growth curves were presented for studies where tumor growth was measurable, serum levels of M protein levels were used as a marker of tumor progression in orthotopic PDX model and Kaplan-Meier curves were used to analyze tumor studies using sBCMA-Fc in combination with bortezomib. Appropriate statistical analysis was used for each experimental study.

Cell lines

Human MM cell lines U266, MM1.R, INA6 and RPMI-8226 cells were maintained in RPMI-1640 media supplemented with 10% fetal bovine serum (FBS) and 1% Penicillin/Streptomycin in standing flasks and a humidified 37 °C, 5% CO_2 incubator. INA6 Cells were supplemented with 2ng/ml of human IL-6 to maintain its growth. All cell lines were generously gifted by Dr. Albert Koong and Dr. Dadi Jiang at the Department of Radiation Oncology, MD Anderson (Houston, TX). IL-6 Reporter HEK 293 Cells were commercially purchased from InvivoGen (Cat. No. hkb-hil6, San Diego, CA.) and BCMA siRNA (SMARTPool Cat. No. L-011217-00-0005) and inducible shRNA (SAMRTvector Cat. No. V3SH7669-230564302) constructs were purchased through GE Dharmacon Horizon (Cambridge, UK). BCMA CRISPR KO (Cat. No. sc-403058) and ATMIN CRISPR KO (sc-411076) constructs were purchased from Santa Cruz Biotechnology (Santa Cruz, CA). All transfection procedure were carried out using Lonza 4D-Nucleofactor Device and kits in accordance with manufacturers protocol (Basal, Switzerland).

Isolation of Human Multiple Myeloma Cells from Patients

Isolation of B-cells from healthy donor and MM patients were performed using EasySep™ Human B-Cell Isolation Kit according to manufacturer's protocol (Cat. No. 17954, Stemcell Technologies, Vancouver, Canada).

Real-Time PCR analysis

RNA was isolated using TRIzol reagent according to the manufacturer's instructions (Invitrogen). RNA was reverse transcribed using cDNA synthesis kit (Biorad, Hercules, CA). Real-time PCR was performed as previously described. Relative expression levels of target genes were normalized against the level of GAPDH expression. Fold difference (as relative mRNA expression) was calculated by the comparative CT method ($2^{Ct(\text{GAPDH RNA–gene of interest})}$).

Primer sequences:

BCMA Fw	TGTTCTTCTAATACTCCTCCTCT
BCMA Rev	AACTCGTCCTTTAATGGTTC
GAPDH Fw	TGCACCACCAACTGCTTAGC
GAPDH Rev	GGCATGGACTGTGGTCATGAG
F Luc Fw	AAGAGATACGCCCTGGTTC
F Luc Rev	TTGTATTCAGCCCATATCGTT
ATMIN Fw	AACAGCACTGCAGTCTCACA
ATMIN Rev	CTGGTCTAGGGATTGGTTGGT
IL6 Fw	TCCACAAGCGCCTTCGGTCC
IL6 Rev	TGTCTGTGTGGGGCGGCTACA

Immunohistochemistry

Tumor tissue slides were deparaffinized with xylene, rehydrated according to standard immunohistochemical methods, and stained with anti-Ki67 primary antibody (Cat. no. SAB5700770; 1:500, Millipore Sigma, Burlington, MA) or no primary (negative controls). Slides were stained using the VECTASTAIN ABC system (Vector Laboratories, Burlingame, CA) and DAB Substrate Kit for Peroxidase (Vector Laboratories) and counterstained with hematoxylin. Ki67 positive tumor cell was quantified according to the average number of positive stained nuclei per field. TUNEL staining was carried out using ApopTag Peroxidase *In Situ* Apoptosis Detection Kit (Cat. no. S7100 Millipore Sigma, Burlington, MA). Experiment performed according to manufacturer's protocol.

Reverse Phase Protein Array (RPPA)

The RPPA was performed by MD Anderson RPPA core as described according to the published protocol.

Enzyme-Linked Immunosorbent Assay (ELISA)

Serum and cell lysate expression of Human APRIL (Cat. no. DY884B, R&D Systems Minneapolis, MN), human BAFF (Cat. no. DBLYS0B, &D Systems Minneapolis, MN), mouse APRIL (Cat. no. MBS738004 My Biosource, San Diego, CA), mouse BAFF (Cat. no. MBLYS0, R&D Systems Minneapolis, MN), Human total IgG (M) protein (Cat. no. BMS2091, ThermoFisher, Waltham, MA), mouse total IgG (M) protein (Cat. no. 88-50400-88, ThermoFisher, Waltham, MA), Human IL-6 (Cat. no. EH2IL6, Invitrogen/ ThermoFisher, Waltham, MA) expressions were detected using commercial ELISA kit listed above according to manufacturer's protocol.

Ribosome Sequencing and Bioinformatic Analysis

Ribo-seq RNA and total RNA libraries of U266 siScramble and U266 siBCMA cells were prepared by TB-SEQ™ (South San Francisco, CA) based on previously published ligation-free ribosome profiling protocol (Hornstein et al. 2016). Briefly, snap frozen cell pellets (100 million cells per sample) were lysed in polysome lysis buffer (20 mM Tris-HCl pH 7.5, 250 mM NaCl, 15mM MgCl2, 1mM DTT, 0.5% Triton X-100, 0.024 U/ml TurboDNase, 0.48 U/ml RNasin, and 0.1 mg/ml cycloheximide). Lysates were centrifuged for 10 minutes at 4C, 14,000 x g. The supernatant was used for the isolation of ribosome bound mRNA, and total mRNA sequencing. SUPERase-In (0.24U/ml) was added to the lysate used for polysome fractionation to prevent RNA degradation.

The sequencing files for ribosome profiling and RNA-Seq data were processed using RiboFlow (29). All source code is freely available at https://github.com/ribosomeprofiling. Briefly, 3' adapter sequence (AAAAAAAAAA) was removed from all reads using cutadapt. The 5' end of each read includes 3 bases from the template switching reaction and also removed before alignment. We used a sequential alignment strategy to first filter out rRNA and tRNA mapping reads followed by mapping to representative isoforms for each as defined in the APPRIS database (50). Next, PCR duplicates were removed from the ribosome profiling data using the 5'end of the sequence alignment coordinates. Finally, the resulting information was compiled into a .ribo file (Ozadam et al. 2020) for downstream analyses.

All statistical analysis were carried using RiboR (29). For quantification of ribosome occupancy, footprints of length between 26 and 30 (both inclusive) nucleotides were used. Metagene plots were generated using the 5' end of each ribosome footprint. Ribosome occupancy and RNA-Seq data was jointly analyzed, and transcript specific dispersion estimates were calculated after TMM normalization (51). To identify genes with differential translation efficiency, we used a generalized

linear model that treats RNA expression and ribosome occupancy as two experimental manipulations of the RNA pool of the cells as previously described (30). The model was fit using edgeR (51) and p-values were adjusted for multiple hypothesis testing using Benjamini-Hochberg correction.

We used an adjusted p-value threshold of 0.05 to define significant differences. R packages cowplot, pheatmap, EnhancedVolcano, ggpubr, ggplot2, and reshape2 were used for analyses and plotting (52).

Polysome Analysis

U266 cells were transfected with siScramble and siBCMA as described. Cells were pelleted and lysed in buffer (20 mM Tris-HCl, pH 7.4, 100 mM NaCl, 5 mM $MgCl_2$, 1 mM DTT, 1 % Triton X-100, 0.1 % NP-40, 100 µg/ml CHX, 20 U/ml TurboDNase I, complete protease inhibitor EDTA-free) in nuclease-free water. After lysis, RNA concentrations were measured using Nanodorop UV spectrophotometer and normalized amounts of RNA were layered onto a sucrose gradient (25-50% sucrose (w/v), 20 mM Tris-HCl, pH 7.4, 100 mM NaCl, 15 mM $MgCl_2$, 100 µg/ml CHX) in nuclease-free water and centrifuged in a SW41Ti rotor (Beckman) for 2.5 hr at 40,000 rpm at 4°C. Sixteen fractions were collected by the Density Gradient Fraction System (Brandel). To each fraction, 0.1 ml of 10 % SDS was added and mixed. 0.1 ml of 3 M NaOAc, pH 5.5 and 0.1 ml of water were added to each SDS containing fraction. For normalization, 500 pg of bioistronic firefly luciferase mRNA was added to each fraction.

Total RNA from each fraction was extracted using acid-phenol:chloroform. Briefly, to each fraction, 900 µl of acid-phenol:chloroform was added and mixed thoroughly. The mixture was heated at 65 °C for 5 min, and centrifuged at 21,000 g for 10 min, RT. The aqueous phase (700 µl)

was removed and precipitated overnight at -80 °C with 700 µl isopropanol and 1.5 µl GlycoBlue Coprecipitate (Invitrogen). The samples were centrifuged at 21,000 g, 30 min, 4 °C, supernatant was discarded, and the RNA pellet was washed twice with 500 µl cold 75 % ethanol. Pellets were dried for 15 min, RT and resuspended in nuclease free water. Total RNA from each fraction was treated with 2 U/µl TurboDNase I, incubated at 37 °C for 30min and column purified using the RNA Clean and Concentrator-5 (Zymo) according to the manufacturer's instructions. RNA was eluted in 6 µl, twice. Except for the first fraction (F1), RNA was pooled from every three subsequent fractions (F2-4, F5-7, F8-10, F11-13, F14-16) and measured using Nanodorop UV spectrophotometer.

For RT-qPCR, 600 ng of purified RNA was used for reverse transcription with the iScript supermix (Bio-Rad) according to the manufacturer's instructions. (Please see qRT-PCR protocol for primer sequences)

Establishing MM PDX model using MM patient specimens

Mononuclear cells were isolated from bone marrow aspirate of Multiple Myeloma patients and inoculated into the left tibia of 5-6 weeks NSG mice. Injection path into the tibia was first established using an empty needle penetrating through the tibia bone guided by X-ray. Once the injection path is confirmed, the empty needle is removed, and X-ray turned off to avoid MM cells exposing to radiation. Patient derived cells were inoculated using a fresh needle and syringe. MM tumor growth was monitored by serum level of human IgG (M) protein since the samples collected predominantly express human IgG. Once the host mice showed successful engraftment marked by steady increase of serum human IgG level, the animal was sacrificed, bone marrow flushed, and mononuclear cells collected for intratibial injection into 2 host mice. This process is repeated

until sufficient N number is reached for each study. 11 patient samples were inoculated, 2 patient samples were successfully propagated for *in vivo* studies.

Mice computerized tomography (CT) scan to confirm MM induced bone degradation

High-resolution micro-CT images were acquired using an *in vivo* micro-CT scanner SkyScan 1276 (Bruker, Billerica, Massachusetts, US) under isoflurane anesthesia. The scanning mode was set as 360°, step-and-shoot scanning without average framing. After each scan, the projection images were reconstructed using the software (NRecon with GPU acceleration, Bruker), followed by converting the set of reconstructed slices to DICOM files (DICOM converter, Bruker).

Establishment of bortezomib resistant MM cell lines

Bortezomib resistant U266, MM1.R and INA6 cells were established by continuous incubation with increasing doses of bortezomib starting from 1nM, to 3, 4, 5, 7, 8 and 10nM. Full recovery of cell viability is confirmed prior to increasing bortezomib to the next dose.

***In vivo* studies**

All animal experiments were reviewed and approved by the Institutional Animal Care and Use Committee (IACUC) at Stanford University. Female NOD-*scid* gamma mice age 6-8 weeks were purchased from the Jackson Laboratory (Stock no. 005557) and used for all *in vivo* analysis throughout the study. Mice were housed in pathogen-free animal facility, kept under constant temperature and humidity and controlled 12 h light-dark cycles. For INA6 and MM1.R as well as MM1.R bortezomib resistant subcutaneous tumor studies (dox-inducible, AAV-sBCMA-Fc), $10x10^7$ cells were injected subcutaneously with 50% growth factor reduced Matrigel (Cat. no. 356230, Corning, NY). Bodyweight and tumor growth were measured 3 times a week until study termination. Animals were terminated upon subcutaneous tumor reaches ethical termination point.

For PDX and MM1.R bortezomib resistant studies, non-terminal bleeding was performed on animals every 14 days for evaluating serum M protein as markers of tumor progression. Animals were terminated once shown signs of physical distress.

In vitro Cell Based Viability Assays

Cell viability was determined with Cell counting hemocytometer or Beckman coulter counter depending on the study. Cells were plated in 96-well plates at a density of 2500 cells (U266 and RPMI-8226) or 3000 cells (MM1.R and INA-6). For sBCMA-Fc treatment, cells were cultured in 1% FCS RPMI media overnight followed by 1 hour of 100ng recombinant APRIL stimulation, increasing doses of sBCMA were added to designated wells. Both APRIL and sBCMA-Fc treatment are replenished every 48 hours until experiment ends.

Immunoblotting

Cell lysates were subjected to sodium dodecyl sulfate polyacrylamide gel electrophoresis, followed by transfer to nitrocellulose membrane. The membranes were then probed with primary Abs against total BCMA (Cat. no. 27724-1-AP, Proteintech, Rosemont, IL), ATMIN/ASCIZ (Cat. no. AB3271-I, Millipore Sigma, Burlington, MA), IL-6 (Cat. no. 21865-1-AP, Proteintech, Rosemont, IL), Pan-Akt (Cat. no. 4691 Cell Signaling Technology, Danvers, MA), pAkt (Cat. no. 4060, Cell Signaling Technology, Danvers, MA), phospho-p44/42 MAPK (Cat. no 4370, Cell Signaling Technology, Danvers, MA), p38 MAPK (Cat. no. 8690 Cell Signaling Technology, Danvers, MA), phospho-eIF4E (Cat. no. 9741, Cell Signaling Technology, Danvers, MA), total eIF4E (Cat. no. 2067, Cell Signaling Technology, Danvers, MA), Phospho-mTOR ser2481 (Cat. no. 2974 Cell Signaling Technology, Danvers, MA), Phospho-mTOR ser2448 (Cat. no. 5536 Cell Signaling Technology, Danvers, MA), total mTOR (Cat. no. 2983 Cell Signaling Technology,

Danvers, MA), Raptor (Cat. no. 2280 Cell Signaling Technology, Danvers, MA), Phospho-Raptor Ser792 (Cat. no. 89146 Cell Signaling Technology, Danvers, MA), Phospho-4EBP1 Thr37/46 (Cat. no. 2855 Cell Signaling Technology, Danvers, MA), Phospho-p70 S6K (Cat. no. 9204 Cell Signaling Technology, Danvers, MA) at 4°C overnight. The blots were then washed and probed with HRP-conjugated anti-goat (no. sc-2020, Santa Cruz Biotechnology Inc.), or HRP-conjugated anti-rabbit (no. A16110, Thermo Fisher Scientific) as appropriate. The blots were developed with Bio-Rad Western C Developing Reagent (no. 170-5060 Bio-Rad) and visualized with Chemidoc digital imager (no. 1708280, Bio-Rad).

Statistical analysis

All cell number, tumor volume, survival and quantification of *in vivo* and *in vitro* studies were conducted using GraphPad Prism software (GraphPad Software Inc, CA). ANOVA with Tukey-Kramer test was used for comparing multiple treatment groups with each other. $P < 0.05$ was considered significant. Repeated measure ANOVA was used for comparing multiple treatment groups measured over time. Statistical analysis of survival curves was conducted for the survival studies. A log-rank (Mantel-Cox) test was performed to compare mean survival among groups; $P \leq 0.05$ was considered statistically significant.

SUPPLEMENTAL MATERIALS

Fig. S1: BCMA signaling is required for MM tumor growth

Fig. S2: Loss of BCMA expression leads to decreased proliferation and increased apoptosis in MM tumors.

Fig. S3: Genome wide ribosome profiling reveals changes in protein translation machinery upon loss of BCMA signaling in MM cells.

Fig. S4: Repeated sBCMA-Fc treatment dose not induce tissue or hematological toxicity in mice.

Data Table S1: RPPA analysis comparing MM cells with siScramble and siBCMA.

Data Table S2: Total RNA-seq analysis MM cells with siScramble and siBCMA.

Data Table S3: Ribosome profiling of translation efficiency in MM cells with siScramble and siBCMA.

REFERENCES

1. Chim CS, Kumar SK, Orlowski RZ, Cook G, Richardson PG, Gertz MA, et al. Management of relapsed and refractory multiple myeloma: novel agents, antibodies, immunotherapies and beyond. *Leukemia.* 2018;32(2):252-62.
2. Durer C, Durer S, Lee S, Chakraborty R, Malik MN, Rafae A, et al. Treatment of relapsed multiple myeloma: Evidence-based recommendations. *Blood Rev.* 2020;39:100616.
3. Raje N, Berdeja J, Lin Y, Siegel D, Jagannath S, Madduri D, et al. Anti-BCMA CAR T-Cell Therapy bb2121 in Relapsed or Refractory Multiple Myeloma. *N Engl J Med.* 2019;380(18):1726-37.
4. Lonial S, Lee HC, Badros A, Trudel S, Nooka AK, Chari A, et al. Belantamab mafodotin for relapsed or refractory multiple myeloma (DREAMM-2): a two-arm, randomised, open-label, phase 2 study. *Lancet Oncol.* 2020;21(2):207-21.
5. Watanabe G, Tanaka N, Ohhira M, Takemura H, and Iwa T. [A successful case of supraarterial myotomy for a myocardial bridging using intra-operative ultrasound technic to locate the intramural coronary artery trees]. *Nihon Kyobu Geka Gakkai Zasshi.* 1988;36(3):411-5.
6. Cohen AD, Garfall AL, Stadtmauer EA, Melenhorst JJ, Lacey SF, Lancaster E, et al. B cell maturation antigen-specific CAR T cells are clinically active in multiple myeloma. *J Clin Invest.* 2019;129(6):2210-21.
7. Zhao WH, Liu J, Wang BY, Chen YX, Cao XM, Yang Y, et al. A phase 1, open-label study of LCAR-B38M, a chimeric antigen receptor T cell therapy directed against B cell maturation antigen, in patients with relapsed or refractory multiple myeloma. *J Hematol Oncol.* 2018;11(1):141.
8. Eaton JS, Miller PE, Mannis MJ, and Murphy CJ. Ocular Adverse Events Associated with Antibody-Drug Conjugates in Human Clinical Trials. *J Ocul Pharmacol Ther.* 2015;31(10):589-604.
9. Gardeney H, Bobin A, Gruchet C, Sabirou F, Levy A, Nsiala L, et al. Three Drug Combinations in the Treatment of Fit Elderly Multiple Myeloma Patients. *J Clin Med.* 2020;9(11).
10. Elnair R, and Holstein S. Treatment Considerations for Transplant-Ineligible Multiple Myeloma. *Oncology (Williston Park).* 2021;35(4):170-82.
11. O'Connor BP, Raman VS, Erickson LD, Cook WJ, Weaver LK, Ahonen C, et al. BCMA is essential for the survival of long-lived bone marrow plasma cells. *J Exp Med.* 2004;199(1):91-8.
12. Chiu A, Xu W, He B, Dillon SR, Gross JA, Sievers E, et al. Hodgkin lymphoma cells express TACI and BCMA receptors and generate survival and proliferation signals in response to BAFF and APRIL. *Blood.* 2007;109(2):729-39.
13. Xu S, and Lam KP. B-cell maturation protein, which binds the tumor necrosis factor family members BAFF and APRIL, is dispensable for humoral immune responses. *Mol Cell Biol.* 2001;21(12):4067-74.
14. Lee L, Bounds D, Paterson J, Herledan G, Sully K, Seestaller-Wehr LM, et al. Evaluation of B cell maturation antigen as a target for antibody drug conjugate mediated cytotoxicity in multiple myeloma. *Br J Haematol.* 2016;174(6):911-22.

15. Tai YT, Mayes PA, Acharya C, Zhong MY, Cea M, Cagnetta A, et al. Novel anti-B-cell maturation antigen antibody-drug conjugate (GSK2857916) selectively induces killing of multiple myeloma. *Blood.* 2014;123(20):3128-38.
16. Tai YT, Acharya C, An G, Moschetta M, Zhong MY, Feng X, et al. APRIL and BCMA promote human multiple myeloma growth and immunosuppression in the bone marrow microenvironment. *Blood.* 2016;127(25):3225-36.
17. Moreaux J, Legouffe E, Jourdan E, Quittet P, Reme T, Lugagne C, et al. BAFF and APRIL protect myeloma cells from apoptosis induced by interleukin 6 deprivation and dexamethasone. *Blood.* 2004;103(8):3148-57.
18. Matthes T, Dunand-Sauthier I, Santiago-Raber ML, Krause KH, Donze O, Passweg J, et al. Production of the plasma-cell survival factor a proliferation-inducing ligand (APRIL) peaks in myeloid precursor cells from human bone marrow. *Blood.* 2011;118(7):1838-44.
19. Tai YT, Li XF, Breitkreutz I, Song W, Neri P, Catley L, et al. Role of B-cell-activating factor in adhesion and growth of human multiple myeloma cells in the bone marrow microenvironment. *Cancer Res.* 2006;66(13):6675-82.
20. Klein B, Tarte K, Jourdan M, Mathouk K, Moreaux J, Jourdan E, et al. Survival and proliferation factors of normal and malignant plasma cells. *Int J Hematol.* 2003;78(2):106-13.
21. Suematsu S, Matsuda T, Aozasa K, Akira S, Nakano N, Ohno S, et al. IgG1 plasmacytosis in interleukin 6 transgenic mice. *Proc Natl Acad Sci U S A.* 1989;86(19):7547-51.
22. Bataille R, Jourdan M, Zhang XG, and Klein B. Serum levels of interleukin 6, a potent myeloma cell growth factor, as a reflect of disease severity in plasma cell dyscrasias. *J Clin Invest.* 1989;84(6):2008-11.
23. Stephens OW, Zhang Q, Qu P, Zhou Y, Chavan S, Tian E, et al. An intermediate-risk multiple myeloma subgroup is defined by sIL-6r: levels synergistically increase with incidence of SNP rs2228145 and 1q21 amplification. *Blood.* 2012;119(2):503-12.
24. Briones J, Timmerman JM, Hilbert DM, and Levy R. BLyS and BLyS receptor expression in non-Hodgkin's lymphoma. *Exp Hematol.* 2002;30(2):135-41.
25. Fragioudaki M, Tsirakis G, Pappa CA, Aristeidou I, Tsioutis C, Alegakis A, et al. Serum BAFF levels are related to angiogenesis and prognosis in patients with multiple myeloma. *Leuk Res.* 2012;36(8):1004-8.
26. Bolkun L, Lemancewicz D, Jablonska E, Kulczynska A, Bolkun-Skornicka U, Kloczko J, et al. BAFF and APRIL as TNF superfamily molecules and angiogenesis parallel progression of human multiple myeloma. *Ann Hematol.* 2014;93(4):635-44.
27. Collier FC, and Jackson P. The precipitin test for Bence-Jones protein. *N Engl J Med.* 1953;248(10):409-14.
28. Ingolia NT, Lareau LF, and Weissman JS. Ribosome profiling of mouse embryonic stem cells reveals the complexity and dynamics of mammalian proteomes. *Cell.* 2011;147(4):789-802.
29. Ozadam H, Geng M, and Cenik C. RiboFlow, RiboR and RiboPy: an ecosystem for analyzing ribosome profiling data at read length resolution. *Bioinformatics.* 2020;36(9):2929-31.
30. Cenik C, Cenik ES, Byeon GW, Grubert F, Candille SI, Spacek D, et al. Integrative analysis of RNA, translation, and protein levels reveals distinct regulatory variation across humans. *Genome Res.* 2015;25(11):1610-21.

31. Becker JR, Cuella-Martin R, Barazas M, Liu R, Oliveira C, Oliver AW, et al. The ASCIZ-DYNLL1 axis promotes 53BP1-dependent non-homologous end joining and PARP inhibitor sensitivity. *Nat Commun.* 2018;9(1):5406.
32. McNees CJ, Conlan LA, Tenis N, and Heierhorst J. ASCIZ regulates lesion-specific Rad51 focus formation and apoptosis after methylating DNA damage. *EMBO J.* 2005;24(13):2447-57.
33. Jurado S, Smyth I, van Denderen B, Tenis N, Hammet A, Hewitt K, et al. Dual functions of ASCIZ in the DNA base damage response and pulmonary organogenesis. *PLoS Genet.* 2010;6(10):e1001170.
34. Rapali P, Garcia-Mayoral MF, Martinez-Moreno M, Tarnok K, Schlett K, Albar JP, et al. LC8 dynein light chain (DYNLL1) binds to the C-terminal domain of ATM-interacting protein (ATMIN/ASCIZ) and regulates its subcellular localization. *Biochem Biophys Res Commun.* 2011;414(3):493-8.
35. Jurado S, Gleeson K, O'Donnell K, Izon DJ, Walkley CR, Strasser A, et al. The Zinc-finger protein ASCIZ regulates B cell development via DYNLL1 and Bim. *J Exp Med.* 2012;209(9):1629-39.
36. Jurado S, Conlan LA, Baker EK, Ng JL, Tenis N, Hoch NC, et al. ATM substrate Chk2-interacting Zn2+ finger (ASCIZ) Is a bi-functional transcriptional activator and feedback sensor in the regulation of dynein light chain (DYNLL1) expression. *J Biol Chem.* 2012;287(5):3156-64.
37. Leszczynska KB, Gottgens EL, Biasoli D, Olcina MM, Ient J, Anbalagan S, et al. Mechanisms and consequences of ATMIN repression in hypoxic conditions: roles for p53 and HIF-1. *Sci Rep.* 2016;6:21698.
38. Leipold D, and Prabhu S. Pharmacokinetic and Pharmacodynamic Considerations in the Design of Therapeutic Antibodies. *Clin Transl Sci.* 2019;12(2):130-9.
39. Marsters SA, Yan M, Pitti RM, Haas PE, Dixit VM, and Ashkenazi A. Interaction of the TNF homologues BLyS and APRIL with the TNF receptor homologues BCMA and TACI. *Curr Biol.* 2000;10(13):785-8.
40. Majithia N, Vincent Rajkumar S, Lacy MQ, Buadi FK, Dispenzieri A, Gertz MA, et al. Outcomes of primary refractory multiple myeloma and the impact of novel therapies. *Am J Hematol.* 2015;90(11):981-5.
41. Kumar SK, Dispenzieri A, Fraser R, Mingwei F, Akpek G, Cornell R, et al. Early relapse after autologous hematopoietic cell transplantation remains a poor prognostic factor in multiple myeloma but outcomes have improved over time. *Leukemia.* 2018;32(4):986-95.
42. Cohen YC, Joffe E, Benyamini N, Dimopoulos MA, Terpos E, Trestman S, et al. Primary failure of bortezomib in newly diagnosed multiple myeloma--understanding the magnitude, predictors, and significance. *Leuk Lymphoma.* 2016;57(6):1382-8.
43. Langerhorst P, Brinkman AB, VanDuijn MM, Wessels H, Groenen P, Joosten I, et al. Clonotypic Features of Rearranged Immunoglobulin Genes Yield Personalized Biomarkers for Minimal Residual Disease Monitoring in Multiple Myeloma. *Clin Chem.* 2021.
44. Ramasamy K, Gay F, Weisel K, Zweegman S, Mateos MV, and Richardson P. Improving outcomes for patients with relapsed multiple myeloma: Challenges and considerations of current and emerging treatment options. *Blood Rev.* 2021:100808.
45. Carpenter RO, Evbuomwan MO, Pittaluga S, Rose JJ, Raffeld M, Yang S, et al. B-cell maturation antigen is a promising target for adoptive T-cell therapy of multiple myeloma. *Clin Cancer Res.* 2013;19(8):2048-60.

46. Ingolia NT, Hussmann JA, and Weissman JS. Ribosome Profiling: Global Views of Translation. *Cold Spring Harb Perspect Biol.* 2019;11(5).
47. Pawlyn C, and Jackson GH. Physicians, paraproteins and progress: diagnosis and management of myeloma. *Br J Hosp Med (Lond).* 2019;80(2):91-8.
48. Kampan NC, Xiang SD, McNally OM, Stephens AN, Quinn MA, and Plebanski M. Immunotherapeutic Interleukin-6 or Interleukin-6 Receptor Blockade in Cancer: Challenges and Opportunities. *Curr Med Chem.* 2018;25(36):4785-806.
49. Trudel S, Lendvai N, Popat R, Voorhees PM, Reeves B, Libby EN, et al. Targeting B-cell maturation antigen with GSK2857916 antibody-drug conjugate in relapsed or refractory multiple myeloma (BMA117159): a dose escalation and expansion phase 1 trial. *Lancet Oncol.* 2018;19(12):1641-53.
50. Rodriguez JM, Rodriguez-Rivas J, Di Domenico T, Vazquez J, Valencia A, and Tress ML. APPRIS 2017: principal isoforms for multiple gene sets. *Nucleic Acids Res.* 2018;46(D1):D213-D7.
51. Robinson MD, and Oshlack A. A scaling normalization method for differential expression analysis of RNA-seq data. *Genome Biol.* 2010;11(3):R25.
52. Kassambara A, and Moreaux J. Analysis of Global Gene Expression Profiles. *Methods Mol Biol.* 2018;1792:157-66.

ACKNOWLEDGMENTS

The authors wish to thank Drs. Vignesh Viswanathan, Dhanya Nambiar, Quynh-Thu Le for sharing experimental reagents. We would like to thank Stanford microscopy facility for electron microscopy imaging, Stanford virus core facility for the production of AAV virus, Stanford animal facility for maintaining animal colonies, Chempartner Shanghai for the production of sBCMA-Fc and Biacore™ analysis, TB-seq for the isolation and preparation of ribosome bound mRNA and the University of Delaware sequencing facility for running ribosome sequencing.

FIGURES

Figure 1

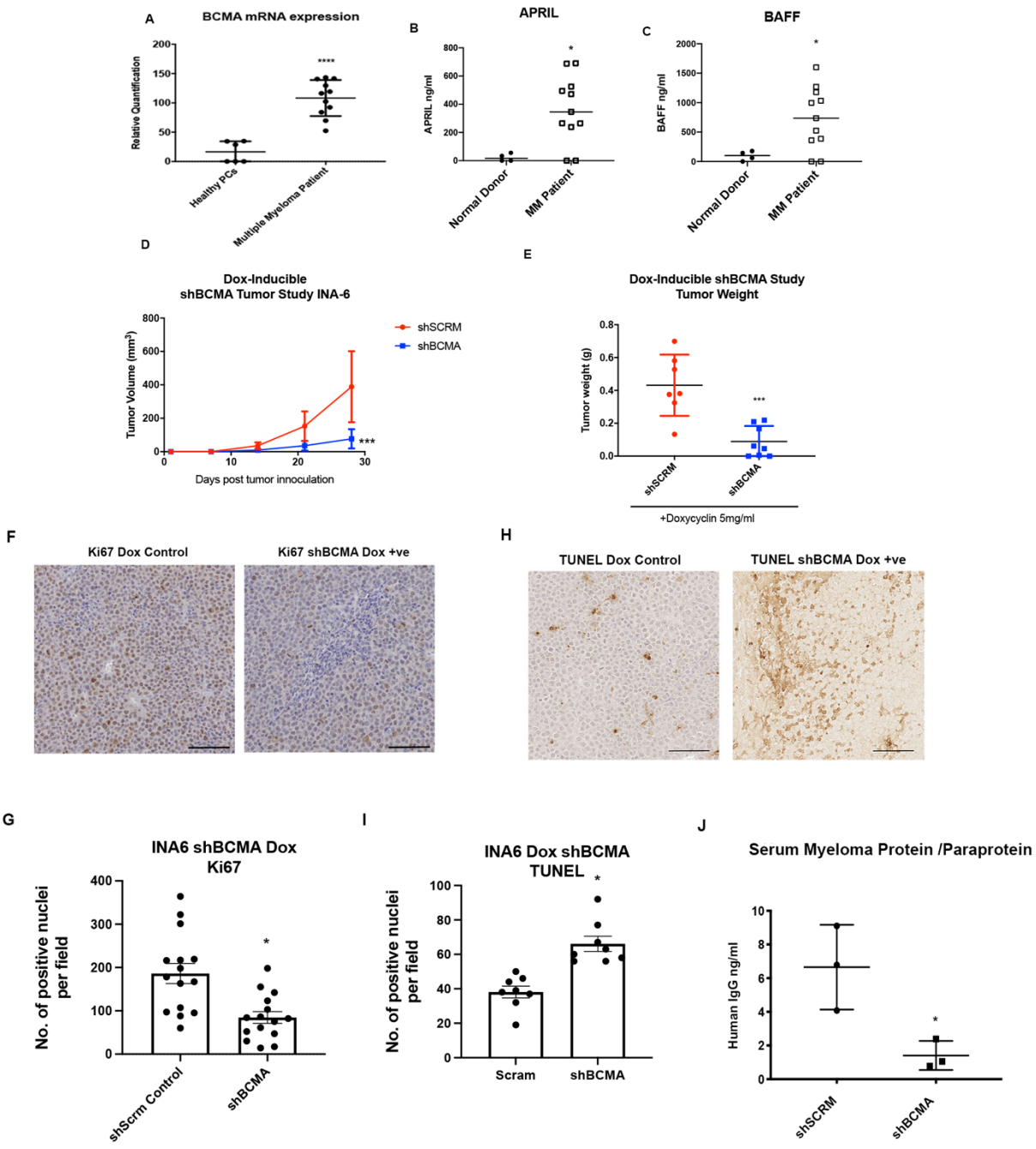

Figure 1: BCMA and its ligands APRIL and BAFF are upregulated in MM and support the growth and survival of MM *in vivo*. (A) BCMA mRNA transcript validated in patient myeloma cells (N=11) and plasma cells harvested from healthy donors (N=6). **(B)** Serum APRIL level detected in MM patients (N=11) compared to healthy donors (N=4) through ELISA. **(C)** Serum BAFF level detected in MM patients (N=11) compared to healthy donors (N=4) through ELISA. **(D)** Subcutaneous tumor growth of INA-6 MM cells with stably transfected doxycycline-inducible BCMA KO shRNA (N=8) or control shRNA (N=7) in 6 weeks old female NSG mice. **(E)** Comparing tumor weights of terminally harvested mice inoculated with doxycycline-inducible shScrm (N=7) and shBCMA (N=8) INA-6 MM tumor cells. **(F)** Representative images of Ki67 positive cells in the harvested tumors of doxycycline-inducible shScrm and shBCMA analyzed by IHC staining. Scale bar 50µm. **(G)** Representative images of TUNEL positive cells in the harvested tumors of doxycycline-inducible shScrm and shBCMA analyzed by IHC staining. Scale bar 50µm. **(H)** Quantitative analysis of Ki67 positive cells in the harvested tumors of doxycycline-inducible shScrm and shBCMA, represented as the average number of positive nuclei per image field. **(I)** Quantitative analysis of TUNEL positive cells in the harvested tumors of doxycycline-inducible shScrm and shBCMA, represented as the average number of positive nuclei per image field. **(J)** Total Human M protein (Paraprotein) detected in the serum of NSG mice inoculated with doxycycline-inducible shScrm and shBCMA human INA-6 MM tumor cells harvested terminally (N=3). Statistical analysis was conducted using One-way ANOVA for comparing between treatment groups and repeated ANOVA for changes occur over-time. P value *=<0.05, **=<0.01. ***=<0.001.

Figure 2

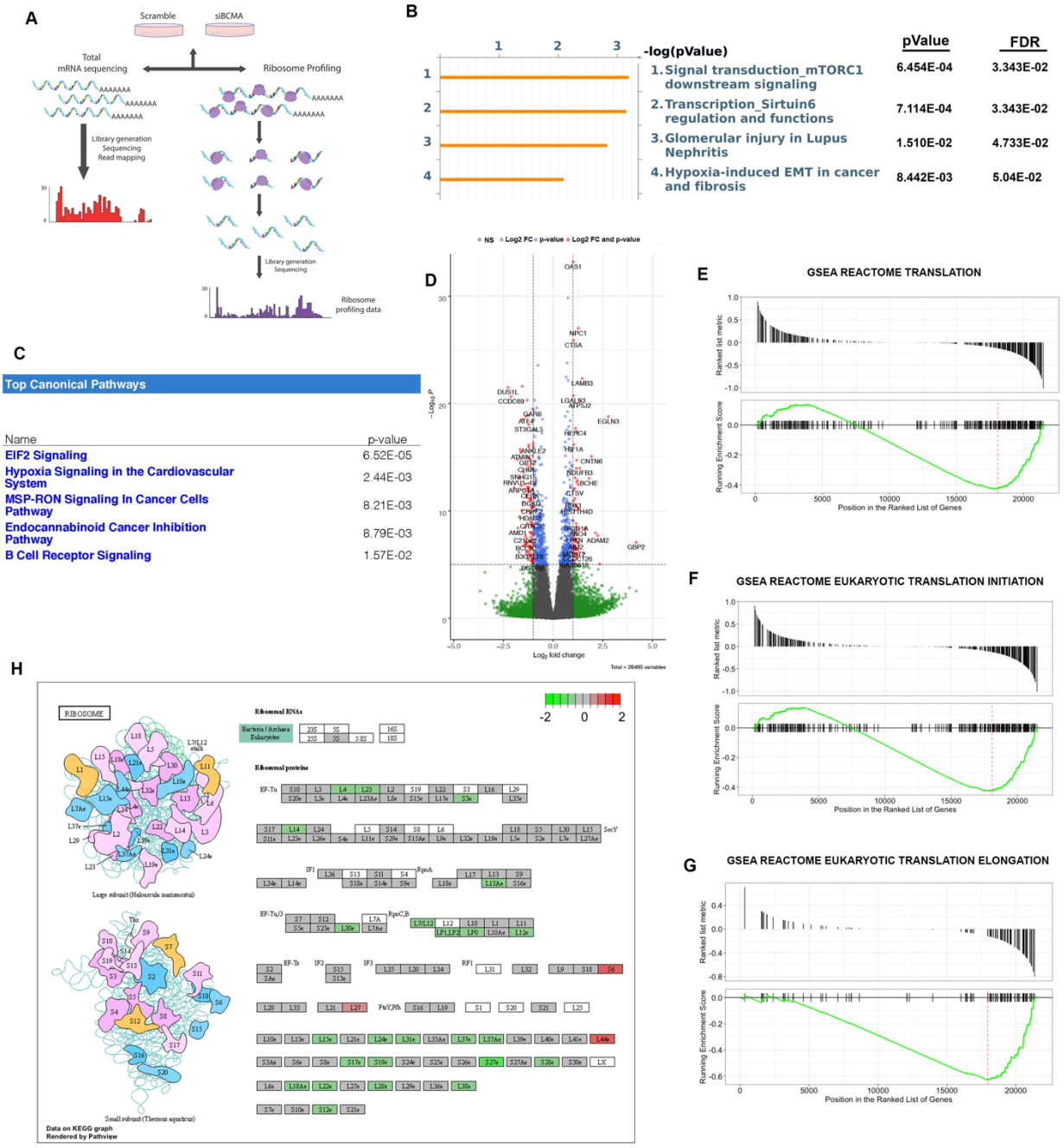

Figure 2: Ribosome profiling identifies BCMA as a master regulator of protein translation machinery in MM. (A) Schematic illustration of ribosome profiling workflow. **(B)** MetaCore analysis revealing top changes in process networks based on Gene Ontology with P-value and FDR**. (C)** Ingenuity Pathway Analysis of RNA-seq showing top five significantly changed

canonical pathways. **(D)** Volcano plot analysis of global changes in of protein translation upon loss of BCMA expression in MM. Not significant (gray), changes in Log_2 FC value (green), significant changes in p-value (red) and changes in both p-value and log FC (red) are presented according to color coding. Left side of the volcano plots shows decrease in target expression upon loss of BCMA, the right side shows negative correlation upon loss of BCMA. **(E)** GSEA REACTOME enrichment analysis showing enriched signatures in associated with protein translation, eukaryotic translation initiation **(F)** and eukaryotic translation initiation **(G)** upon BCMA loss. **(H)** Graphic illustration of large ribosome subunits (top) and small ribosome subunits (bottom). Each subunit showing changes in translation abundance upon BCMA loss. Decreased expression (green), no change (gray) or increased expression (red).

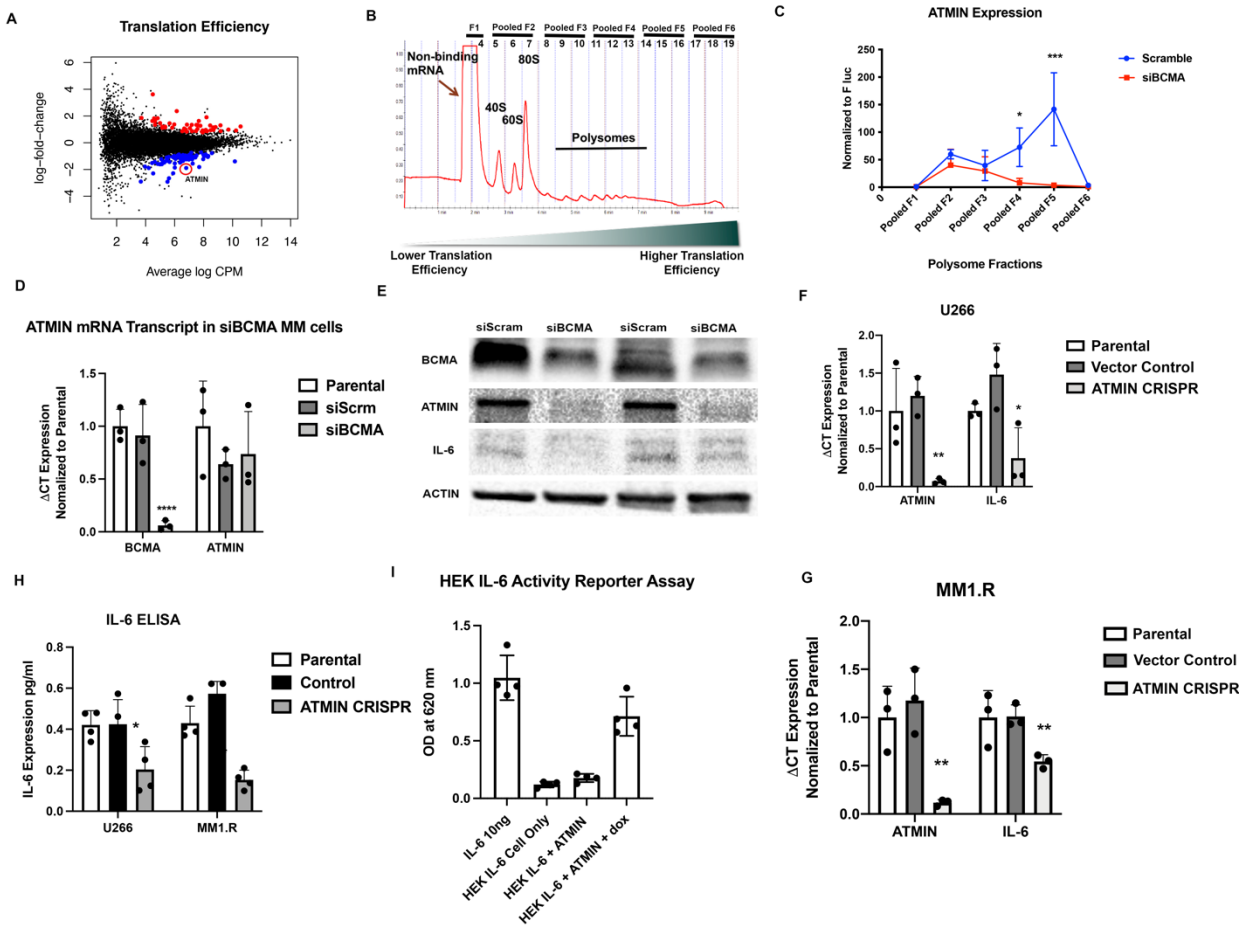

Figure 3: BCMA signaling regulates IL-6 through modulating the translation efficiency of ATMIN. (A) Translation Efficiency analysis of MM cells upon loss of BCMA expression. Significant outcomes are colored in blue (downregulation) and red (upregulation) with ATMIN highlighted with red circle. **(B)** Representative polysome profile of U266 MM cells fractionated by ultracentrifugation through a 10%-50% sucrose gradient. Fractions were pooled for mRNA analysis. **(C)** Relative abundance of ATMIN mRNA expression analyzed in each of the pooled polysome fraction comparing U266 siScramble with siBCMA MM cells. Each biological sample were performed in triplicates. **(D)** Total mRNA expression of BCMA and ATMIN examined in parental, siScrm and siBCMA U266 MM cells. Each biological sample were performed in triplicates. **(E)** Western blotting analysis of total protein ATMIN and IL-6 expression of ATMIN

and IL-6 examined in siScrm and siBCMA MM cells. **(F)** Total mRNA expression of ATMIN and IL-6 examined in U266 parental, vector control and ATMIN CRISPR knockout MM cells. Each biological sample were performed in triplicates. **(G)** Total mRNA expression of ATMIN and IL-6 examined in MM1.R parental, vector control and ATMIN CRISPR knockout MM cells. Each biological sample were performed in triplicates. **(H)** Secreted IL-6 levels in the supernatants of U266 ATMIN CRIPSR KO MM cells compared to parental and ATMIN CRISPR Control in both U266 and MM1.R MM cells. ELISA performed in quadruplicate. **(I)** IL-6 mediated signaling reporter activity assay using a HEK293-derived cell line with the genes encoding human IL-6 receptor (IL-6R) and signal transducer and activator of transcription 3 (STAT3). This reporter cell line is further transfected with a doxycycline inducible ATMIN expression construct. Statistical analysis was conducted using T test and one way ANOVA for comparing between treatment groups. P value *=<0.05, **=<0.01. ***=<0.001.

Figure 4

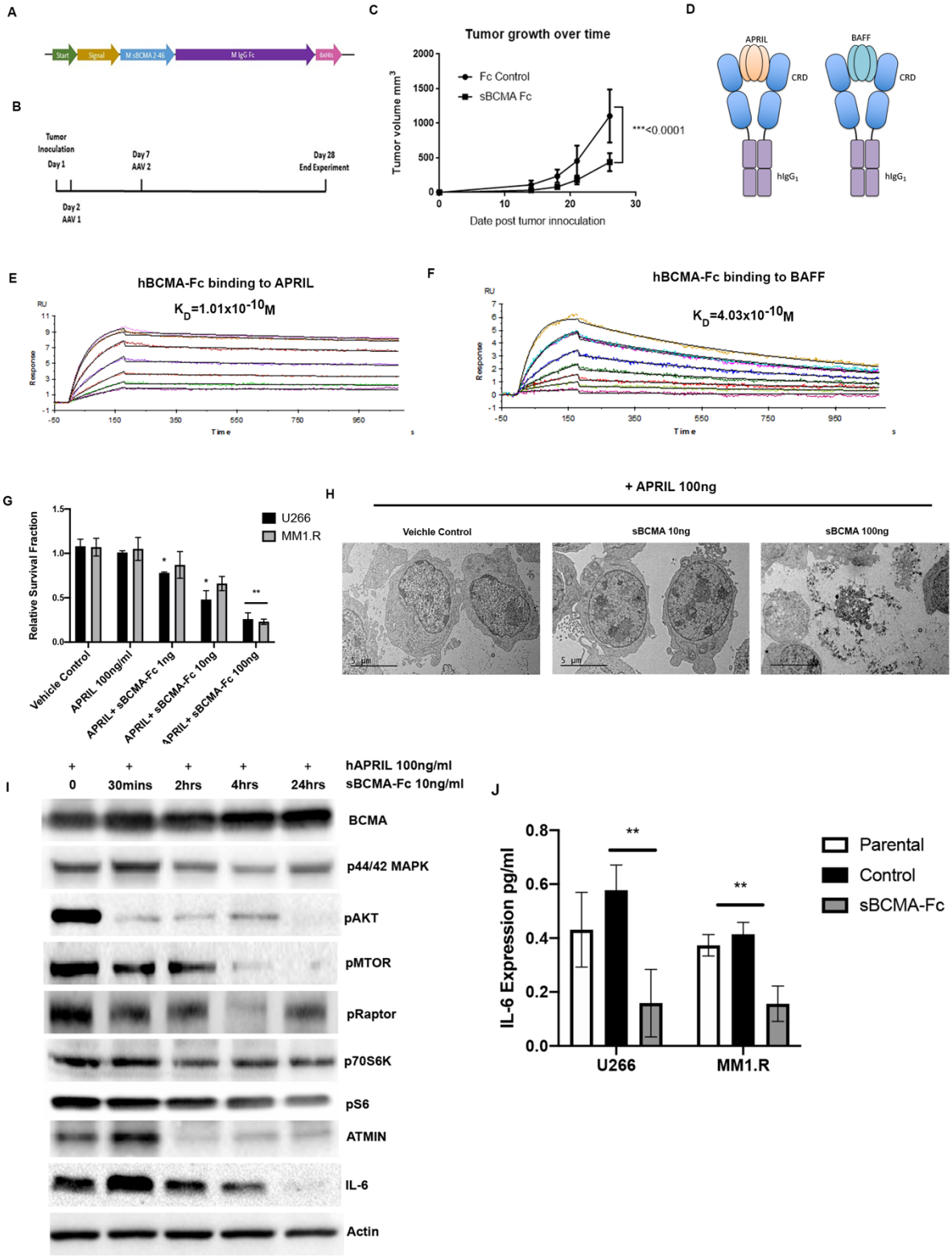

Figure 4: Soluble BCMA decoy receptor as a targeted treatment through neutralizing APRIL and BAFF. (A) Illustrative design of AAV virus construct expressing mouse soluble BCMA amino acid no. 2 to 46 (M sBCMA 2-46) fused with mouse IgG Fc. **(B)** Schematic protocol of AAV dosing in animals inoculated with MM1.R MM tumors. **(C)** Subcutaneous tumor growth of MM1.R MM cells in mice dosed with AAV sBCMA Fc (N=8) or AAV Fc control (N=8) in 6 weeks old female NSG mice. **(D)** Schematic illustrations of recombinant human sBCMA-Fc binding to human ARPIL and BAFF. **(E)** SPR Biacore® analysis of binding constant (K_D) between sBCMA-Fc to ARPIL. Each line represents the binding kinetic of a single concentration of analyte (APRIL) tracked over-time. **(F)** SPR analysis of binding constant (K_D) between sBCMA-Fc to BAFF. Each line represents the binding kinetic of a single concentration of analyte (APRIL) tracked over-time. **(G)** sBCMA-Fc dose-dependent, cell-titer blue cytotoxicity assay validating the in vitro cell survival in the presence of increasing doses of sBCMA-Fc and APRIL (100ng/ml) in U266 and MM1.R MM cells. Cells were maintained in a low 3% FCS to reduce possible growth stimulation mediated through other growth factors present in FCS. Each sample was performed in triplicates. **(H)** Representative Transmission Electron Microscopy images of U266 MM cells treated with vehicle control, sBCMA-Fc at 10ng/ml and sBCMA-Fc at 100ng/ml in the presence of APRIL (100ng/ml). Scale bar 5mM. **(I)** Representative western blot analysis of changes in protein expression downstream of the BCMA signaling upon treatment with 10ng/ml sBCMA-Fc at multiple time point with APRIL added as signaling activator. **(J)** Secreted in IL-6 levels in the supernatants of U266 and MM1.R MM cells treated with 100ng/ml of sBCMA-Fc. ELISA performed in triplicates in each experimental group. Statistical analysis was conducted using T test and one way ANOVA for comparing between treatment groups. Repeated ANOVA used for changes in tumor growth over-time. P value *=<0.05, **=<0.01. ***=<0.001

Figure 5

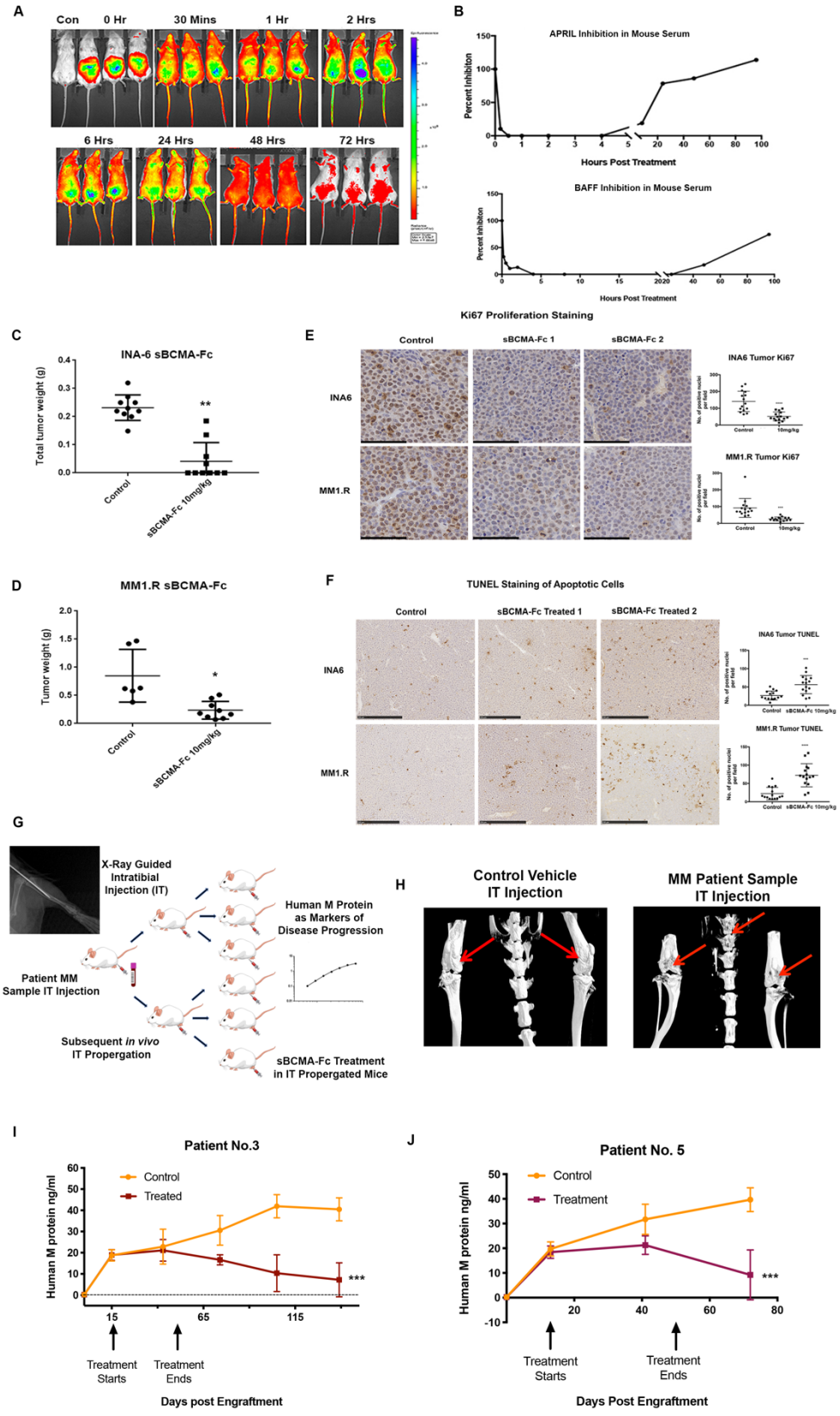

Figure 5: sBCMA-Fc treatment effectively inhibits MM tumor growth through the neutralization of APRIL and BAFF. (A) Pharmacokinetic analysis of sBCMA-Fc labeled with Alexa Fluor® 488 after given a single dose of 10mg/kg IP were imaged over-time. **(B)** Serum level of APRIL (top panel) and BAFF (bottom panel) in mouse blood after a single dose of sBCMA-Fc 10mg/kg given IP. Each data point represents the mean of two animals collected at the same time point. **(C)** Terminal tumor weight of mice inoculated with INA-6 MM tumors and treated with vehicle control or 10mg/kg of sBCMA-Fc. **(F)** Terminal tumor weight of mice inoculated with MM1.R MM tumors and treated with vehicle control or 10mg/kg of sBCMA-Fc. **(E)** Representative images of Ki67 positive cells in the vehicle control and sBCMA-Fc treated INA-6 (top panels with quantification on the top right) and MM1.R (bottom panels with quantification on the bottom left) MM tumors analyzed by IHC staining. Scale bar 100μm. **(F)** Representative images of TUNEL positive cells in the vehicle control and sBCMA-Fc treated INA-6 (top panels with quantification on the top right) and MM1.R (bottom panels with quantification on the bottom left) MM tumors analyzed by IHC staining. Scale bar 100μm. **(G)** Schematic illustrations of *in vivo* MM PDX propagation. Patient tumor cells were isolated from patient bone marrow biopsies and inoculate intra-tibialy into NSG mice. Successful engraftment confirmed through the detection of human M protein in mouse serum. PDX were subsequently propagated *in vivo* using intratibial inoculation and treated with vehicle control or sBCMA-Fc for 28 days. Human M protein in mouse serum is continuously monitored over-time as a marker of tumor progression. **(H)** Representative CT scans of mice tibias, femurs and vertebrates that have being inoculated with control (left) or MM PDX tumor cells (right). Osteolytic bone degradation was observed in MM PDX injected animal (red arrows on the right image) but not in the control injected animal (red arrows on the left image). **(I)** Human M protein in mouse serum detected in animals successfully engrafted with

MM cells from patient No. 3 showing reduction in Human M protein level post sBCMA-Fc treatment (N=8) compared to vehicle control (N=7). **(J)** Human M protein in mouse serum detected in animals successfully engrafted with MM cells from patient No. 5 showing reduction in Human M protein level post sBCMA-Fc treatment (N=10) compared to vehicle control (N=10). Statistical analysis was conducted using T test and one way ANOVA for comparing between treatment groups. Repeated ANOVA used for changes in tumor growth over-time. P value *=<0.05, **=<0.01. ***=<0.001.

Figure 6

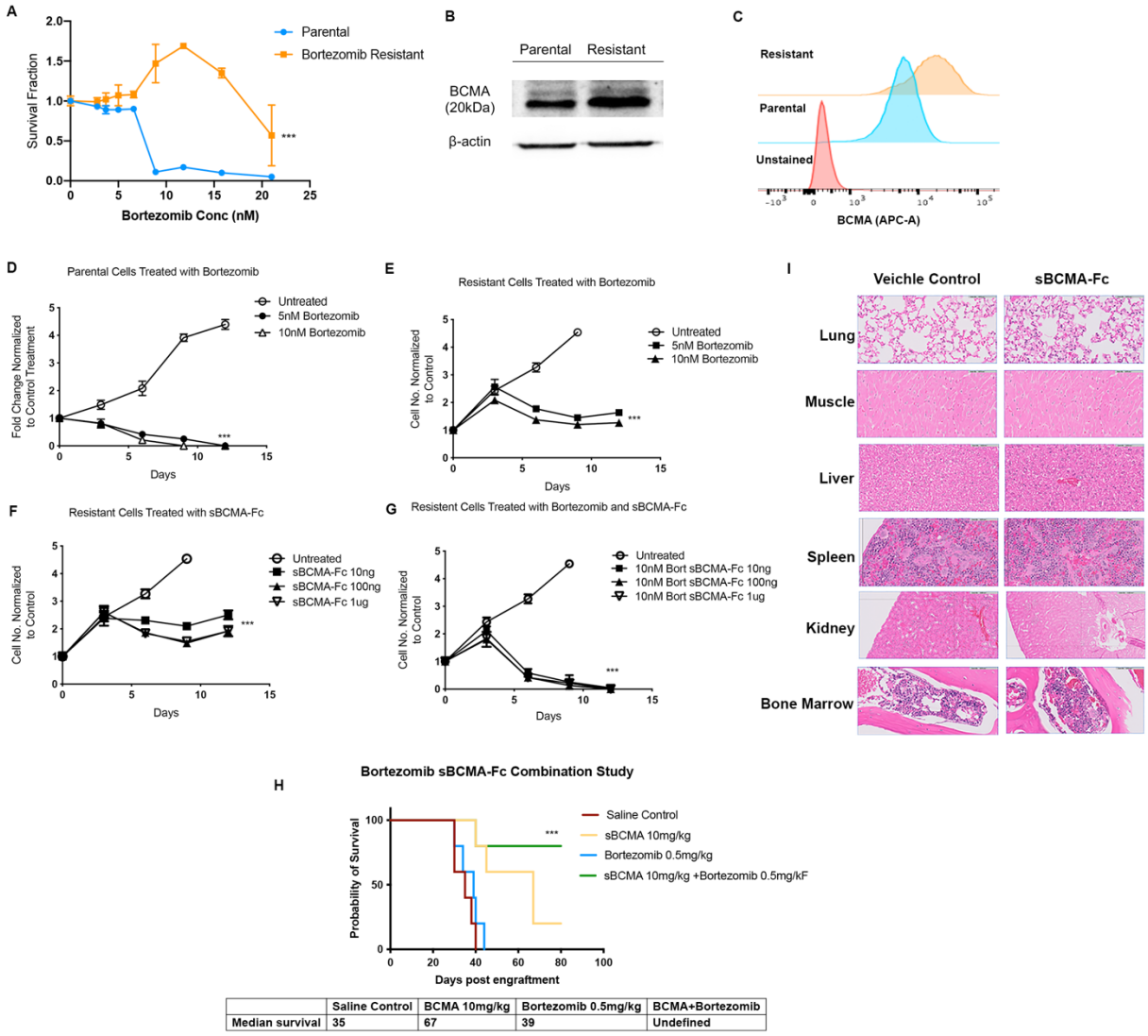

	Saline Control	BCMA 10mg/kg	Bortezomib 0.5mg/kg	BCMA+Bortezomib
Median survival	35	67	39	Undefined

Figure 6: sBCMA-Fc treatment re-sensitizes bortezomib resistant MM and can be safely used in combination with SOC. (A) *In vitro* dose-dependent survival analysis of U266 parental and bortezomib resistant cell treated with increasing doses of bortezomib. **(B)** Representative western blot analysis showing elevated expression of BCMA in bortezomib resistant U266 MM cells. **(C)** BCMA expression on U266 parental and bortezomib resistant cells analyzed by flow cytometry. **(D)** *In vitro* cell survival analysis of U266 parental cells treated with increasing doses of bortezomib over-time. Each data points represents technical triplicate of a single experiment.

(E) *In vitro* cell survival analysis of U266 bortezomib resistant cells treated with increasing doses of bortezomib over-time. Each data points represent technical triplicate of a single experiment. **(F)** *In vitro* cell survival analysis of U266 bortezomib resistant cells treated with increasing doses of sBCMA-Fc over-time. Each data points represent technical triplicate of a single experiment. **(G)** *In vitro* cell survival analysis of U266 bortezomib resistant cells treated with 10nM of bortezomib in combination with increasing doses of sBCMA-Fc over-time. Each data points represent technical triplicate of a single experiment. **(H)** Kaplan Meier survival plot of NSG mice orthotopically inoculated with MM1.R MM tumors and treated with vehicle control, sBCMA-Fc 10mg/kg, bortezomib 0.5mg/kg and combination of sBCMA-Fc 10mg/kg and bortezomib 0.5mg/kg. sBCMA-Fc were dosed IP every 48 hours and bortezomib were dosed via oral gavage daily. Animals terminated once tumor reaches ethical end point. Median survival of each experimental group listed below. **(I)** Representative H & E staining images of organ tissues harvested from non-tumor bearing mice treated with sBCMA-Fc at 10mg/kg every 48 hours for 28 days. Stained sections were analyzed by a board-certified veterinary pathologist. Scale bar 100μm. Statistical analysis was conducted using One-way ANOVA for comparing between treatment groups and repeated ANOVA for changes occur over-time. Kaplan Meier estimator was calculated for survival curves. P value *=<0.05, **=<0.01. ***=<0.001.

FUNDINGS

The Silicon Valley Foundation (A.J.G)

The Sydney Frank Foundation (A.J.G)

The Kimmelman Fund (A.J.G)

Medical Research Council (MRC) UK Grant (A.J.G)

AUTHORS CONTRIBUTIONS

Conceptualization: YRM, CC, DJ, KM, EXZ, ML, PA, ACK, AJG

Methodology: YRM, CC, DJ, KM, GCL, HZ, KT, ML, PA, AL

Investigation: YRM, CC, DJ, KM, GCL, HZ, KT, AD, JX, EXZ

Fund acquisition: AJG

Project administration: YRM AJG

Supervision: YRM, ACK, AJG

Writing: YRM, CC, DJ, AJG

COMPETING INTEREST

Authors declare that they have no competing interests.

DATA AND MATERIAL AVAILABILITY

All data associated with this study are in the paper or the Supplementary Materials. All reagents will be made available to members of the research community after completion of a material transfer agreement. Reagent requests should be directed to A.J.G (giaccia@stanford.edu, amato.giaccia@oncology.ox.ac.uk.) and copied to Y. R. M (ymiao@stanford.edu)